RGSA – Revista de Gestão Social e Ambiental
ISSN: 1981-982X
Submission date: 08/12/2024
Acceptance date: 10/14/2024
DOI: https://doi.org/10.24857/rgsa.v18n11-218
Organization: Interinstitutional Scientific Committee
Chief Editor: Ana Carolina Messias de Souza Ferreira da Costa
Assessment: Double Blind Review pelo SEER/OJS

VEGETATION DENSITY MAPPING OF URBAN SOLID WASTE LANDFILL COVERAGE USING VEGETATION INDEXES OBTAINED WITH UAV

Alexandre Felipe Bruch[1]
Karina Retzlaff Camargo[2]
Marciano Carneiro[3]
Gabriel Fragali de Castro[4]
Vinicius Klumb[5]
Talison Luis de Britto Monte[6]
Isabel Cordeiro Borges[7]

ABSTRACT

Objective: The objective of this study is to map the vegetation cover of a municipal solid waste landfill using high-resolution vegetation index images obtained with UAV, as a tool for geotechnical monitoring.

Theoretical Framework: The theoretical framework describes the state of the art of vegetation indexes, starting from the first proposal of NVDI by Rouse *et al.* (1973), through to the NDWI by McFeeters (1996). Additionally, it presents the method of representing radiometric variables, considering that these indexes operate based on the ratio between spectral bands, which are displayed within intervals ranging from -1 to +1.

Method: The study used a UAV equipped with MAPIR multispectral camera to capture images of the landfill. NDVI and NDWI indexes were applied to assess vegetation health and coverage. Field control points determined with GNSS-RTK, along with protogrametry software, ensured mapping accuracy, creating high-resolution orhomosaics for monitoring and determining vegetation indexes.

Results and Discussion: The results indicate variation in vegetation cover, revealing areas of exposed soil ang vegetation at different stages of vigor, from senescence to full growth. The NDVI and NDWI indexes highlighted regions with water stress and soil exposure, demonstrating the effectiveness of the method in environmental and geotechnical monitoring.

Conclusions: It is concluded that the use of UAVs and vegetation indexes are effective for monitoring vegetation health and landfill stability, enanbling the identification of erosion areas and the need for vegetation cover restoration.

Keywords: NDVI, NDWI, Vegetation Cover, Aerial Survey.

[1] Universidade Federal de Pelotas, Pelotas, Rio Grande do Sul, Brazil. E-mail: afbruch@gmail.com
Orcid: https://orcid.org/0000-0003-1734-6799
[2] Universidade Federal do Rio Grande, Rio Grande, Rio Grande do Sul, Brazil.
E-mail: karinacamargo@gmail.com Orcid: https://orcid.org/0000-0002-6427-329X
[3] Universidade Federal do Rio Grande do Sul, Porto Alegre, Rio Grande do Sul, Brazil.
E-mail: marciano.carneiro@ufrgs.br Orcid: https://orcid.org/0000-0003-4436-1935
[4] Universidade Federal de Pelotas, Pelotas, Rio Grande do Sul, Brazil.
E-mail: gabrielfragali.castro2015@gmail.com Orcid: https://orcid.org/0009-0007-4474-6866
[5] Universidade Federal de Pelotas, Pelotas, Rio Grande do Sul, Brazil. E-mail: viniklumb@gmail.com
Orcid: https://orcid.org/0009-0005-0859-4223
[6] Universidade Federal de Pelotas, Pelotas, Rio Grande do Sul, Brazil. E-mail: talisonluisbritto@gmail.com
Orcid: https://orcid.org/0009-0009-1859-2845
[7] Universidade Federal de Pelotas, Pelotas, Rio Grande do Sul, Brazil. E-mail: isabel.engeo@gmail.com
Orcid: https://orcid.org/0009-0002-1308-6651

MAPEAMENTO DA DENSIDADE DA VEGETAÇÃO DE COBERTURA DE UM ATERRO DE RESÍDUOS URBANOS ATRAVÉS DE ÍNDICES DE VEGETAÇÃO OBTIDOS COM VANT

RESUMO

Objetivo: O objetivo deste estudo é realizar o mapeamento da vegetação de cobertura de um aterro sanitário de RSU através de imagens de índices de vegetação de alta resolução obtidas com VANT, como ferramenta de monitoramento geotécnico.

Referencial Teórico: O referencial teórico descreve o estado da arte dos índices de vegetação, desde a primeira proposta de NDVI apresentada por Rouse et al. (1973), passando pelo NDWI de McFeeters (1996). Além disso, apresenta o método de representação das variáveis radiométricas, visto que são índices operados entre razão de bandas espectrais, as quais são apresentados em intervalos que variam de -1 a +1.

Método: O estudo utilizou um VANT com câmera multiespectral MAPIR para capturar imagens do aterro sanitário. Foram aplicados os NDVI e NDWI para avaliar a saúde e cobertura da vegetação. Pontos de controle em campo determinados com GNSS-RTK e programas de fotogrametria garantiram a precisão no mapeamento, criando ortomosaicos de alta resolução para o monitoramento e determinação dos índices de vegetação.

Resultados e Discussão: Os resultados indicam variações na cobertura vegetal, revelando áreas de solo exposto e vegetação em diferentes estágios de vigor, desde senescência até crescimento pleno. Os índices NDVI e NDWI destacaram regiões com estresse hídrico e exposição de solos, demonstrando a efetividade do método no monitoramento ambiental e geotécnico.

Conclusões: Conclui-se que o uso de VANTs e índices de vegetação são eficazes para o monitoramento da saúde vegetal e estabilidade de aterros, permitindo identificar áreas de erosão e necessidade de recomposição da cobertura vegetal.

Palavras-chave: NDVI, NDWI, Vegetação de Cobertura, Aerolevantamento.

MAPEO DE LA DENSIDAD DE VEGETACIÓN DE LA COBERTURA DE UN VERTEDERO DE RESIDUOS SÓLIDOS URBANOS MEDIANTE ÍNDICES DE VEGETACIÓN OBTENIDOS CON UAV

RESUMEN

Objetivo: El objetivo de este estudio es realizar el mapeo de la vegetación de cobertura de um vertedero de resíduos sólidos urbanos mediante imágenes de índices de vegetación de alta resolución com UAV, como herramineta de monitoreo geotécnico.

Marco Teórico: El marco teórico describe el estado del arte de los índices de vegetación, desde la primeira propuesta de NDVI presentada por Rouse *et al.* (1973), passando por el NDWI de McFeeters (1996). Además, presenta el método de representación de las variables radiométricas, considerando que son índices operados entre la razón de bandas espectrales, las cuales se representam em intervalos de varían de -1 a +1.

Método: El studio utilizo un UAV equipado con una câmara multiespectral MAPIR para capturar imágenes del vertedero. Se aplicaron los índices NDVI y NDWI para evaluar la salud y la cobertura de la vegetación. Los puntos de control em campo determinados com GNSS-RTK, junto com software de fotogrametria, garantizaron la precisión del mapeo, creando ortomosaicos de alta resolución para el monitore y la determinación de índices de vegetación.

Resultados y Discusión: Los resultados obtenidos revelaron [sintetizar los principales resultados de la investigación]. En la sección de discusión, estos resultados se contextualizan a la luz del marco teórico, destacando las implicaciones y relaciones identificadas. En este apartado también se consideran posibles discrepancias y limitaciones del estudio.

Conclusiones: Se concluye que el uso de UAVs e índices de vegetación es eficaz para el monitoreo de la salud de la vegetación y la estabilidad de los vertederos, permitiendo identificar áreas de erosión y la necessidade de recomposición de la cobertura vegetal.

Palabras clave: NDVI, NDWI, Vegetación de Cobertura, Aerolevantamiento.

1 INTRODUCTION

The increasing generation of Municipal Solid Waste (MSW) is a direct consequence of population and urbanization growth and current consumption patterns, representing on of the main environmental challenges for cities worldwide. With the rising amount of waste produced daily, public managers face the difficult task of ensuring proper collection, treatment, and final disposal of these materials. In urban centers, final disposal in sanitary landfills stands out as the primary alternative, as it allows for controlled and technically feasible management of waste that cannot be recycled or reused.

Although sanitary landfills are the ideal destination for MSW that cannot be recycled or reused, there are records of geotechnical issues in these sites, such as landslides and even collapses, as reported by Nagalli (2005), Nascimento (2007), Schuler (2010), Benevuto (2012, 2016 and 2019), and Shimazaki (2017). Therefore, geotechnical monitoring is crucial, as the mapping of landslide risk areas on slopes, as stablished in NBR 11.682 (ABNT, 2006) and, specifically for sanitary landfills, in NBR 8.419 (ABNT, 1992), especially in areas where the vegetation cover does not show full integrity (Benvenuto, 2012).

In this context, the maintenance of vegetation cover on MSW sanitary landfills has been impacted by climate change, and its causes have been the subject of growing debate, driven by recent extreme events such as prolonged droughts, heatwaves, and intense rainfall, which have become more severe and frequent (Ganho, 2019; Fernandes *et al.*, 2021; Ayandale *et al.*, 2022; Costa *et al.*, 2023). These events impact multiple aspects of human well-being, resulting in significant consequences for communities and ecosystems (Espindola and Ribeiro, 2020). In particular, the increase in rainfall intensity, caused by changes in the hydrological regime, has directly influenced soil water erosion processes, exacerning problems related to soil loss and environmental degradation (Borrelli *et al.*, 2020).

In this context, remote sensing and photogrametry techniques have stood out as essential tools for environmental studies. The analysis of vegetation targets through vegetation indexes allows for a detailed assessment of vegetation cover, providing valuable data on its conditions and variations (Côrrea *et al.*, 2018). Nery *et al.* (2014) emphasize that these indexes are

fundamental for understanding the biophysical and structural characteristics of plants, and that in the context of water erosion, the analysis of vegetation cover is crucial for understanting soil degradation processes. Studies on water erosion are particularly relevant for sustainable management and monitoring of soil loss, allowing for the monitoring of erosive processes, their remediation, and the restoration of vegetation cover, which stabilizes the impacted surface (Silva *et al.*, 2011).

Therefore, the main objetctive of this paper is to map the vegetation cover of as MSW sanitary landfill using vegetation index images as a tool for geotechnical monitoring. The research also presents results from areas where vegetation is experiencing water stress and vegetative vigor conditions.

2 THEORETICAL FRAMEWORK

Since the 1960s, humanity has been capturing images of planet Earth through orbital satellites, with the primary aim of gathering information for environmental monitoring, agriculture, geological mapping, metereology, urban planning, and more (Liu, 2007; Jensen, 2009). Given the vast availability of data obtained from orbital satellites, various methodologies have been developed for processing images and extracting information about Earth's surface.

One of the first methodologies utilizing remote sensing date are radiometric or vegetation indexes. According to Ji *et al.* (2011), vegetation indexes yield dimensionless measures of spectral reflectances calculates though algebraic operations such as ratios, differences, and normalized differences between two or more bands, aiming to quantify the biophysical characteristics of vegetation. According to Jensen (2009), vegetation indexes consist of a dimensionless radiometric measure, indicating the photosynthetic activity of vegetation, chlorophyll content in plants, biomass accumulation, development state, among other characteristics (Jensen, 2009).

In 1972, Person and Miller developed the Ratio Vegetation Index (RVI), the first vegetation index described in the literature (Liu, 2007). This index is based on the theory that green leaves absorb electromagnetic radiation in the invisible region and reflect it in the near-infrared range. Although this wavelength range is significantly affected by atmospheric interference, it has shown good results as an indicator of crop growth and biomass stock (Liu, 2007; Jensen, 2009; Ji *et al.*, 2011).

The most well-known and widely discussed vegetation index in the literature was proposed by Rouse *et al.* (1973) and is called the Normalized Difference Vegetation Index

(NDVI). This index is calculated by the difference in reflectance between two regions of the electromagnetic spectrum, normalized by the ratio of visible and near-infrared bands. In the invisible spectrum, the red wavelength range is used (Liu, 2007).

O NDVI developed by Rouse *et al.* (1973) became widely used because it offers significant advantages, partially eliminating atmospheric interferences, as well as radiometric and geometric disturbances, along with variations in solar and viewing angles (Holben, 1986). As a normalized index, its results range from -1 to +1, where negative values refers to clouds and values close to zero represent exposed soil or areas without vegetation. Positive values reflect areas with vegetation, with higher values indicating denser or more vigorously growing vegetation (Hunt *et al.*, 2010).

The Normalized Difference Water Index (NDWI), proposed by McFeeters (1996), was developed to map and assess water resource data, such as identifying drainage and monitoring flooded areas (Menon *et al.*, 2015). With the advancement of high-resolution sensors, particularly airbone sensors, it became possible to generate NDWIs for determining water scarcity and/or water stress indexes, as well as monitoring changes in vegetation water content (Lu *et al.*, 2024). The NDWI also produces normalized indexes ranging from -1 to +1, directly reflecting the water content present in vegetation.

3 STUDY AREA

This research was conducted at a municipal solid waste sanitary landfill in the municipality of Rio Grande, Rio Grande do Sul state, along the BR-392 highway (Figure 1). From the center of Rio Grande, heading toward the city of Pelotas, the landfill is located approximately 25 km away, in the Vila da Quinta District. The landfill cell is bounded by the coordinates 337.860 to 378.130 meters East and 6.455.470 to 6.455.703 meters North. Both boundaries and coordinates are referenced to the Universal Transverse Mercator Projection, Zone 22S, and the Geocentric Reference System for the Americas – SIRGAS 2000.

Figure 1

Location map of the study area.

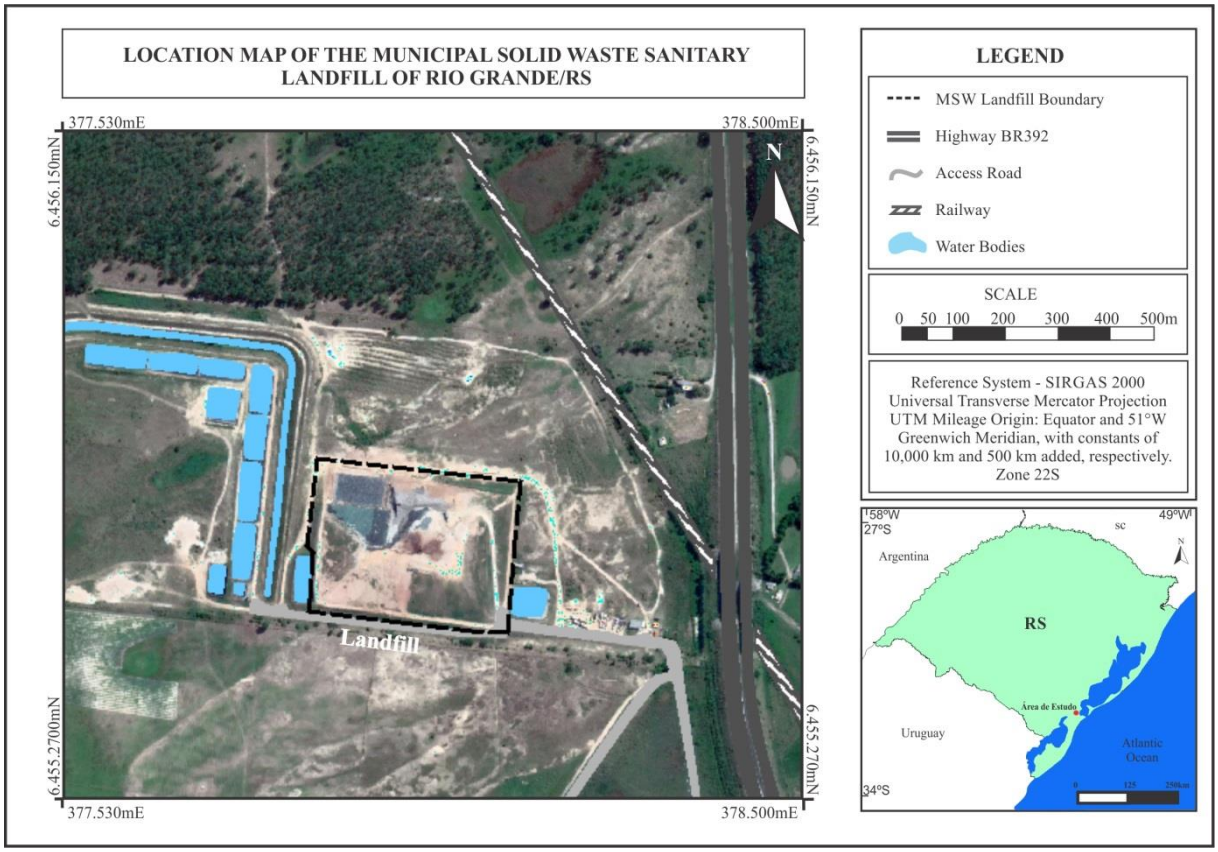

The landfill is located within the geological-geomorphological unit known as the Coastal Plain of Rio Grande do Sul (CPRS), which corresponds to the surface sediments of the Pelotas Basin (PB). The region has relatively flat to level terrain morphology, formed during Quaternary period through the Lagoon-Barrier System (Villwock *et al.*, 1986). The geological-geomorphological substrate unit of the landfill is classified as Aeolian Beach Deposits, belonging to Barrier II, according to Villwock *et al.* (1986), with fine sands, well-sorted, with parallel-plane and cross-bedding, medium to fine sand, well-rounded and well-sorted. Its genesis is related to the reworking of material by winds following the marine regression that defined Barrier II (Tomazelli and Villwock, 1991). Altitudes are generally no greater than 17 m, and slopes are bellow 2%. The landfill cover soil consists of compacted clay material, which has low permability. Rainfall is considered well-distributed, with an average of 120 mm per month and approximately 1.400 mm annually (BRUCH, 2020).

4 MATERIALS AND METHODS

4.1 MATERIALS

For conducting the aerial survey in this research, a DJI multirotor Unmanned Aerial Vehicle (UAV), model Phantom 4 Advanced, was chosen. To obtain the NDVI, a Mapir multispectral camera, model Survey 3W, was used, equipped with imaging sensors in the greem (G-550 nm), red (R-660 nm), and near-infrared (NIR-850 nm) wavelengths. For radiometric correction of the images generated by the Mapir Survey 3W camera, the diffuse reflectance calibration target V2 was chosen, which performs atmospheric interference corrections, providing reflectance percentages (Table 1).

A pair of Global Navigation Satellite System (GNSS) receivers with real-time kinematic (RTK) corrections was also used. The receivers are Emilid brand, model Reach RS2, with L1, L2 bands and multi-constellation support (GPS, GLONASS, BeiDou, and Galileo).

Table 1

Equipment used of field survey.

Instrument	Specifications
	Flight wight: 1368 g Flight autonomy: 28 minutes Maximum radio transmitter range: 5 km Battery: LiPo4s de 5870 mAH Camera: 20 Mega pixels CMOS sensor Maximum Photo Resolution 5472 x 3648 pixels Spatial Postioning: GPS + GLONASS
	Weigth with battery: 76 g Sensor: Sony Exmor R IMX117 Focal distance: 35 mm Maximum Photo Resolution: 4000 x 3000 pixels HFOV: 41º (horizontal) ISO: 50/100/200/400/Automático Capture speed: RAW+JPG (3 seconds/photo); JPG (2 seconds/photo) Spatial Positioning: GPS+GLONASS
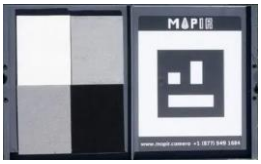	Dimensions (HxWxD): 3,175x254x318 (mm) Radiometric intervals 0/128/255 Identification: QR Code Registration Height: 0,5 a 10 m Calibration: Espectrofotômetro Shimadzu Recognition: MCC ou Mapir Cloud

4.2 METHODS

First, the aerial survey project was developed, aiming to delineate the study area. Then, to increase the accuracy of the aerial survey, a fligh plan was created using the free DroneDeploy software, as shown in Table 2.

Table 2

Flight plan for UAV mapping.

Project	Specifications
	Flight altitude: 60 m Lateral overlap of flight lines: 65% Frontal everlap of photos: 75% Fligth azimuth: 85º Maximum speed: 5 m/s Camera orientation: Nadir Spatial resolution: 1,2 cm/pixel Fligth time: 12 minutes and 57 seconds

Given the inacuracies generated by the UAV's GNSS receiver, 12 control points (CPs) were used in the field (Table 3). The three-dimensional position of a CP is recorded after ambiguities are resolved and a Fixed solution is obtained, with horizontal precisions of 7 mm + 1 ppm and vertical precisions of 14 mm + 1 ppm. After the field survey, the Base position log was compressed and sent for post-processing to correct errors using the Precise Positioning Point (PPP) system from the Brazilian Institute of Geopraphy and Statistics (IBGE). The geodetic reference system used was SIRGAS 2000, and the projetction was the Universal Transverse Mercator, Zone 22S.

Table 3

Control points defined in the field and used in photogrammetric processing.

CP Materialization	Point	Coord. X (mE)	Coord. Y (mN)	Coord. Z (m)
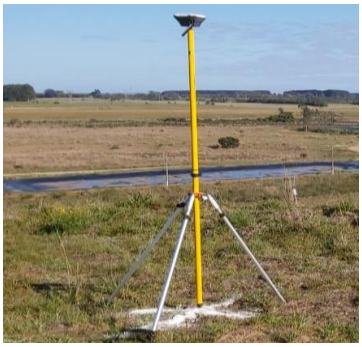	1	378033.546	6455570.730	39.327
	2	377792.999	6455503.777	18.379
	3	377806.576	6455529.050	14.201
	4	377596.199	6455537.176	16.232
	5	377673.687	6455825.667	13.050
	6	377834.141	6455576.858	17.304
	7	377797.147	6455650.239	18.790
	8	378088.960	6455851.157	18.442
	9	378300.868	6455614.742	18.733
	10	378289.812	6455462.015	19.775
	11	378107.637	6455477.188	23.058
	12	378086.183	6455629.970	30.584

With the CPs materialized in the field, the position of the V2 diffuse reflectance calibration target was set 5 meters from the UAV's takeoff point, allowing for its identification in various images captured by the Mpair Suervey 3W camera. The calibration target was identified in 14 images, with 3 images showing standard radiometric intervals within the acceptable threshold. The Mapir Camera Control (MCC) software was used to apply vignete correction (low field), sensor response correction, and white balance.

Vignette correction brightens the outer perimeter of image pixels, which appear darker due to lens optics. Sensor response correction adjusts for sensor sensitivity differences caused by the low-pass noise filter. Finally, white balance harmonizes the minimum and maximum radiometric values recorded using the "gray world" technique (Mapir, 2024). The calibrated images are then exported in Joint Phoographic Experts Group (JPEG) format.

For photogrammetric processing, the software Metashape Professional, developed by Agisoft, was used, employing a combination of Structure-from-Motion and Multi-View Stereo algorithms (SfM-MVS). The SfM-MVS technique enables the generation of high-precision three-dimensional (3D) digital models from a set of two-dimensional (2D) images (Carrivick *et al.*, 2016). According to Bruch *et al.* (2019), the SfM-MVS technology allows for the processing of arbitrary images with varying overlap, provided there are homologous points in distinct images. Additionally, Metashape includes an automatic routine for recognizing images captured by different UAVs and cameras, allowing for the creation of high spatial resolution orthomosaics through mosaicking techniques based on radiometric similarities between images or positional coordinates (Taddia *et al.*, 2020; Zhou *et al.*, 2020).

Thus, a visual analysis of image quality was first conducted, followed by importing the images into Metashape. The next step involves aligning the images (Figure 2), where the software defines the parameters of the camera used, the Principal Point (pp), and the photo rotation. Then, the 12 CPs are added to the images by visually identifying the targets materialized in the field. Subsequently, the photogrammetric parameters of the Mapir Survey 3W camera are calibrated, including adjustments to focal length (f), principal point in x and y (ppx, ppy), third-order symmetrical radial distortion coefficients (k1, k2, k3), and tangential distortion coefficients (P1, P2). Finally, the dense point cloud and photogrammetric orthomosaic are generated. The orthomosaic was exported in JPEG format for generating vegetation indexes in Quantum GIS (QGIS 3.28).

Figure 2

Sparse cloud of homologous points.

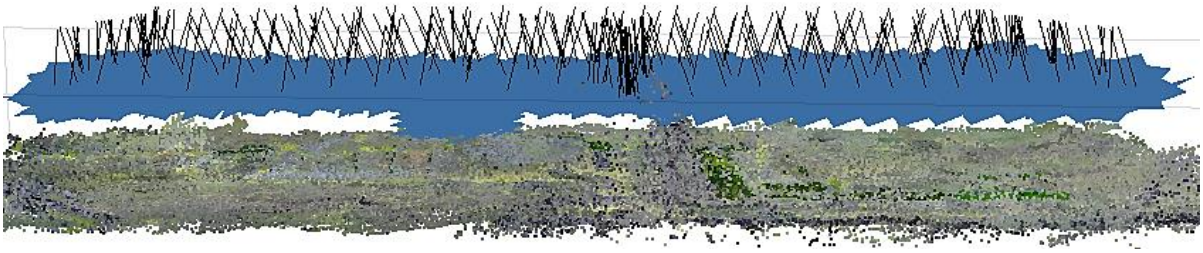

The vegetation indexes were generated according to the NDVI proposed by Rouse *et al.* (1973), as described in Equation 1, and the NDWI proposed by McFeeters (1996), presented in Equation 2. The equations were applied using the Raster Calculator tool available in QGIS 3.28. The equations were applied using the Raster Calculator tool available in QGIS 3.28.

$$NDVI = \left(\frac{NIR-RED}{NIR+RED}\right) \quad (1)$$

where:

NDVI = Normalized Difference Vegetation Index;
RED = Spectral band with red wavelength;
NIR = Spectral band with near-infrared wavelength.

$$NDWI = \left(\frac{GREEN- NIR}{GREEN + NIR}\right) \quad (2)$$

where:

NDWI= Normalized Difference Water Index;
GREEN = Spectral band with green wavelength;
NIR = Spectral band with near-infrared wavelength.

5 RESULTS AND DISCUSSION

The analysis of vegetation density mapping results for the MSW landfill cover shows the presence of discontinuities, interpreted as grass matting and the initial development of gullies in various stages of evolution. Thus, even with a visual inspection of the orthomosaic (Figure 3), created using spectral bands in the visible region (B1-Blue, B2-Green, B3-Red), it

is possible to observe roughness and variations in the vegetation density covering the landfill. The identification and mapping of erosive processes through UAV aerial surveys are widely recognized, with Verdonk (2015), Wang *et al*. (2016), Báčová *et al*. (2019), and Julian and Nunes (2020) attributing these results to the high spatial resolution of the orthomosaic and contrast correction (white balance) from the automatic radiometric calibration of the small-format camera, enabling the delineation of small targets.

Figure 3

Orthomosaic with gully delineation on the landfill surface.

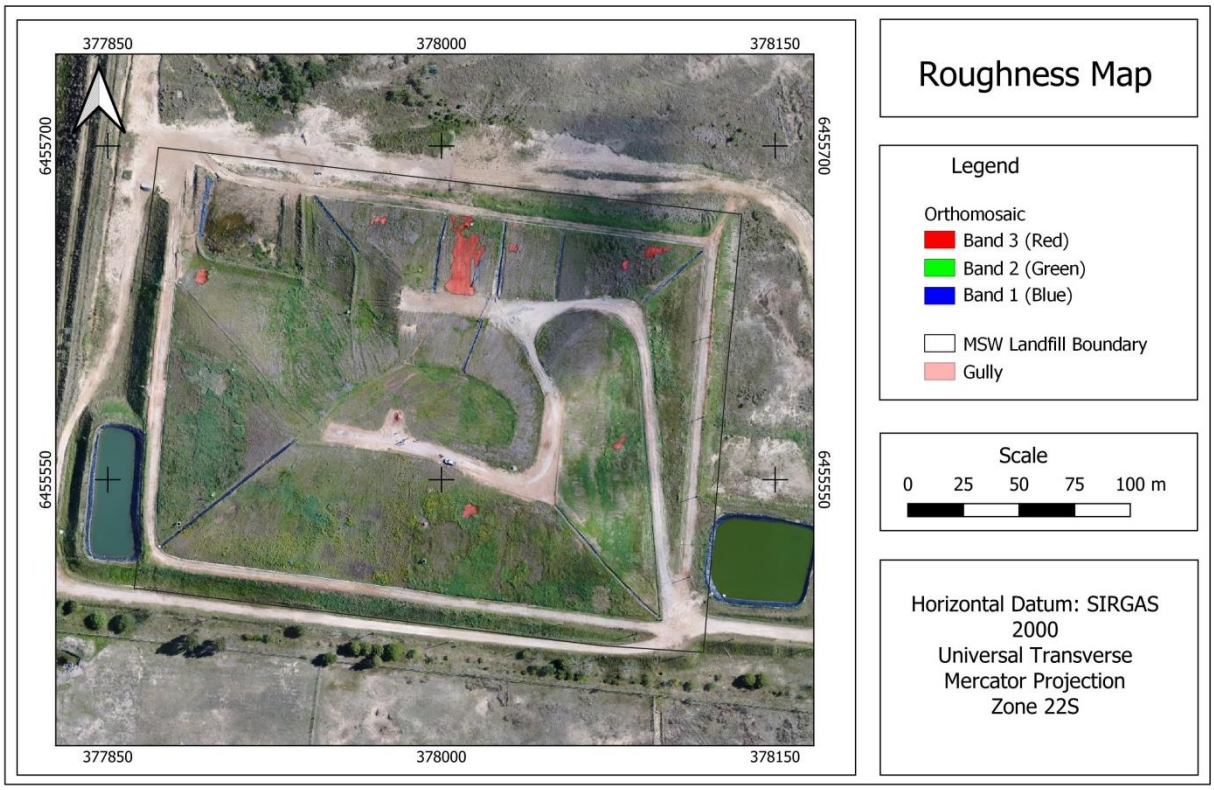

To determine and interpret the targets within the NDVI, class segmentation of radiometric response intervals was performed. Figure 4 shows the NDVI in 5 classes, and Figure 5 presents the histogram that generated the segmentation of intervals among the 5 described targets. Notably, the NDVI matrix produced 16,457,144 pixels due to the high spatial resolution generated by the Mapir camera, with a flight plan altitude of 60 m and a Ground Sample Distance (GSD) of 1.2 cm.

The NDVI results ranged between -0.320 and 0.160. NDVI digital values between -0.320 and -0.101 correspond to exposed soil areas, mainly the access roads to landfill cells and areas where gullies with bifurcations and knickpoints (Guerra, 2005) are already present,

similar to erosion processes in agriculture described by Meinen and Robinson (2020). Similar results were found by Beniaich *et al*. (2022) in olive orchards and large areas of exposed soil between green lines. Ayalew *et al*. (2020) also reported similar radiometric indexes in active erosion processes monitored with NDVI. These areas require soil layer restoration as well as replanting and re-establishment of vegetation cover for the landfill.

Figure 4

NDVI indexes segmented by targets.

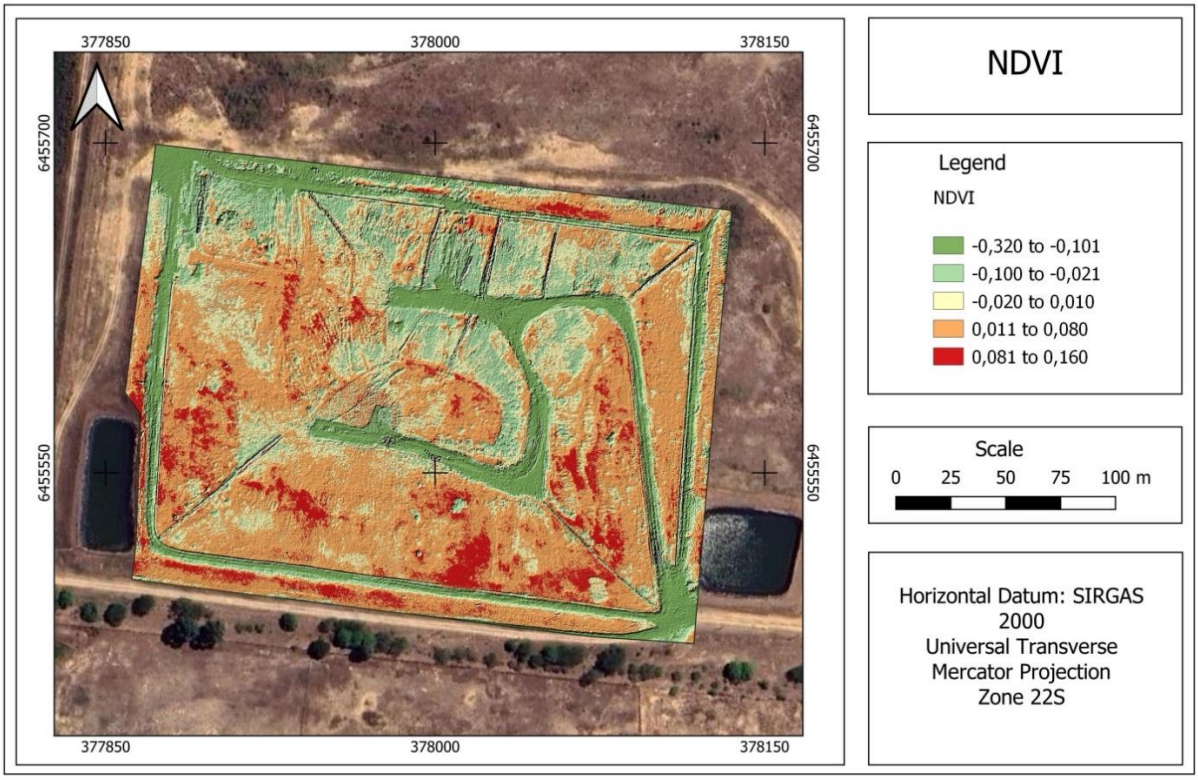

Figure 5

Histograms with class distribution for NDVI and NDWI intervals.

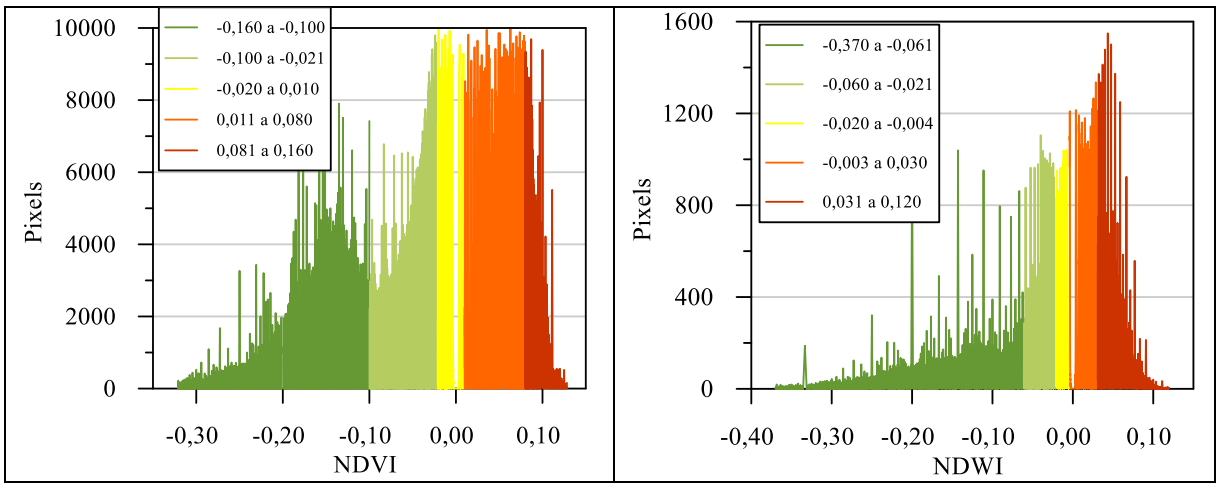

In areas where vegetation shows a state of senescence, indicating a regressive process in vegetative vigor, the NDVI radiometric response ranged from -0.100 to -0.021. In these areas, vegetation is in a state of cellular deterioration and in the final stage of vegetative vigor. Due to the low capacity for water retention and absorption, vegetation in senescence contributes minimally to reducing surface runoff during high rainfall events, as it has a reduced leaf area for flow retention.

NDVI results between -0.020 and 0.010 correspond to areas where grasses from the *Poaceae* family are regaining vegetative vigor, with the fibrous root system absorbing nutrients and water, restoring the coleorrhiza. The stems and leaves covering the soil are responsible for these NDVI responses, with similar results found by Zúñiga and Vásquez (2021) and Jara (2022).

In areas where the vegetative vigor of grasses in the *Poaceae* family is at its peak, NDVI results showed responses ranging from 0.011 to 0.080. These intervals align with other studies, such as those by Ayalew *et al*. (2020), Zúñiga and Vásquez (2021), Jara (2022), and Beniaich *et al*. (2022), which demonstrate that healthy ground vegetation, particularly grasses, is indicated by minimum NDVI values between 0.01 and 0.10 when determined using ultra-high-resolution, radiometrically corrected cameras.

Finally, the highest NDVI responses, ranging from 0.081 to 0.160, were found in invasive cover vegetation, meaning species that have proliferated but were not part of the original vegetation cover project. These are generally Dodonaceae viscosa shrubs intermixed with Poaceae grasses, forming a mosaic-like surface. Invasive species in cover areas are common and generally do not exacerbate erosive processes, providing good soil stability and fixation (Guerra, 2005).

The NDWI results (Figure 6) followed the radiometric responses of the NDVI, with access roads showing the lowest radiometric responses, ranging from -0.370 to -0.06. In areas where vegetation is in a state of senescence, NDWI values ranged from -0.060 to -0.021. This low radiometric response of vegetation indicates significant water stress, as noted in studies by Silva *et al*. (2011) and Marion *et al*. (2021).

Areas where vegetation begins to recover vigor and intracellular water saturation, despite leaves still showing water deficit, yielded NDWI results between -0.020 and -0.004. In areas of full vegetative vigor, NDWI values ranged from -0.003 to 0.030, similar to the findings of Oliveira *et al*. (2010) and Silva *et al*. (2011). This class represents the largest area mapped in the NDVI and NDWI survey (Table 4).

Figura 6

Índices NDWI segmentados por alvos.

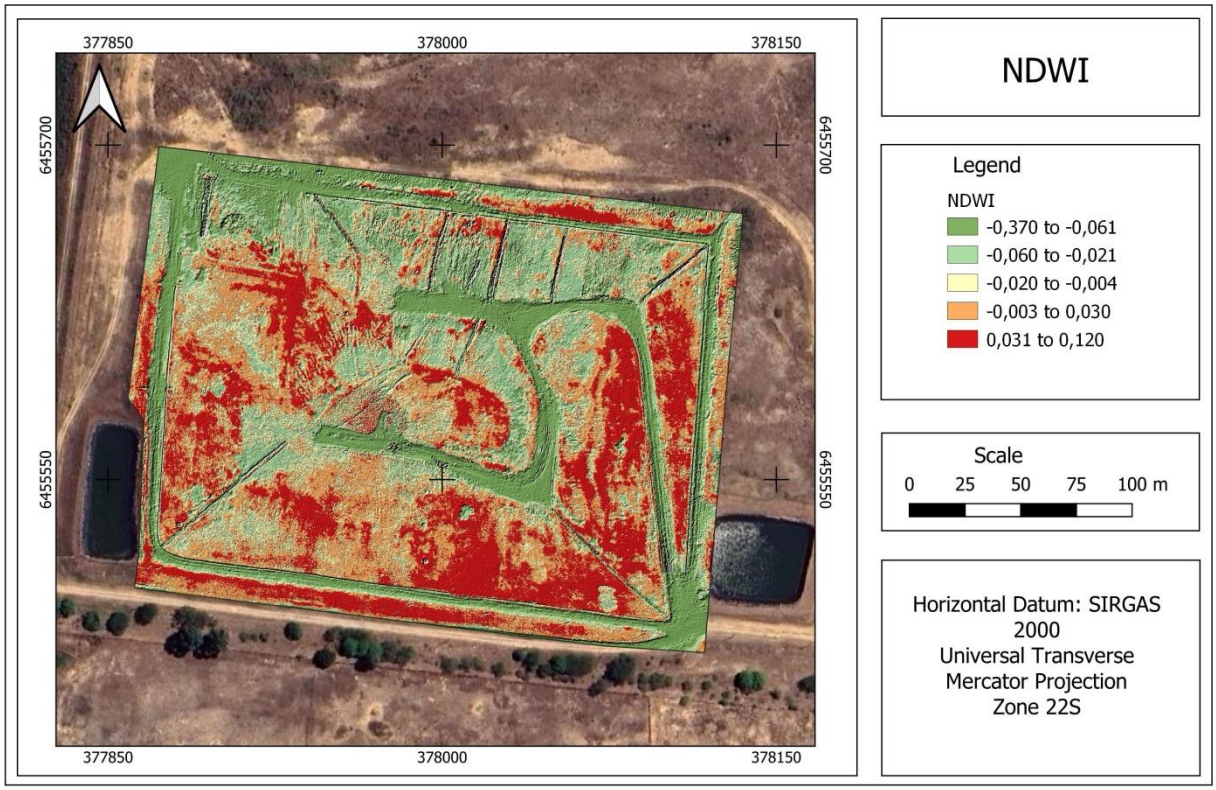

Table 4

Calculated áreas for diferente NDVI and NDWI classes.

NDVI	Area (m²)	NDWI	Area (m²)
-0,320 to -0,101	7.809,36	-0,370 to -0,061	11.238,00
-0,100 to -0,021	7.508,43	-0,060 to -0,021	8.094,94
-0,020 to 0,010	8.815,23	-0,020 to -0,004	5.851,75
0,011 to 0,080	23.431,86	-0,003 to 0,030	15.178,52
0,081 to 0,160	3.673,95	0,031 to 0,120	10.875,62
Total	51.238,83		51.238,83

Finally, NDWI results between 0.031 and 0.120 correspond to polygons with invasive species that exhibit higher water saturation in the aerial system, in addition to full vegetative vigor. Similar to the NDVI, these areas generally consist of shrubs interspersed with grasses, forming a mosaic-like vegetative carpet.

6 CONCLUSION

The study conducted vegetation density mapping of cover in a municipal solid waste (MSW) landfill using vegetation indexes generated by unmanned aerial vehicles (UAVs) and

specific sensors. In response to the environmental challenges posed by waste accumulation, particularly in landfills, the study highlighted the importance of vegetation as a stabilizing factor for landfill cover material, thereby reducing geotechnical risks such as landslides and erosion. The adopted methodology involved using multispectral cameras mounted on UAVs to capture images in the visible and near-infrared ranges, from which NDVI and NDWI vegetation indexes were calculated, both consistent with recent studies.

NDVI revealed vegetation cover variations ranging from -0.320 to 0.160, with specific ranges associated with different vegetation conditions, from exposed soil areas requiring vegetation cover restoration to areas with healthy and invasive vegetation. These data are essential for identifying and monitoring erosive processes and assessing the health and vigor of vegetation, which are crucial for the effectiveness and longevity of the landfill as a waste disposal solution. NDWI also provided relevant insights into the vegetation's water condition, indicating levels of water stress in various areas of the landfill.

Furthermore, the study underscored the effectiveness of using UAVs in high-resolution photogrammetry for continuous landfill monitoring, providing detailed information and allowing for prompt interventions in areas with degraded vegetation. In conclusion, this technology contributes significantly to environmental monitoring and sustainable landfill management, supporting the preservation of cover material integrity and enhancing geotechnical monitoring.

REFERENCES

ABNT - Associação Brasileira de Normas Técnicas. (1991). Estabilidade de Taludes. NBR-11.682. Rio de Janeiro: ABNT 39p.

ABNT - Associação Brasileira de Normas Técnicas. (1992). Apresentação de projetos de aterros sanitários de resíduos de sólidos urbanos. NBR-8.419. Rio de Janeiro: ABNT 7p.

Ayalew, D. A.; Deumlich, D.; Sarapatka, B.; Doktor, D. (2020). Quantifying the sensitivity of NDVI-based C-factor estimation and potential soil erosion prediction using spaceborne earth observation data. *Remote Sens*. v. 12, 1136. https://doi.org/10.3390/rs12071136.

Ayanlade, A.; Oluwaranti, A.; Ayanlade, O. S.; Borderon, M.; Sterly, H.; Sakdapolrak, P.; Jegede, M. O.; Weldemariam, L. F.; Ayinde, A. F. O. Extreme climate events in sub-Saharan Africa: A call for improving agricultural technology transfer to enhance adaptive capacity. *Climate Services*. v. 27. 2022. https://doi.org/10.1016/j.cliser.2022.100311

Bácová, M.; Krása, J.; Devátý, J.; KAVKA P. A. (2019). GIS method for volumetric assessments of erosion rills from digital surface models. *European Journal of Remote Sensing*, v. 52, S1, p. 96-107. https://doi.org/10.1080/22797254.2018.1543556.

Beniaich, A.; Silva, M. L.; Guimarães, D. V.; Avalos, F. A.; Terra, F. S.; Menezes, M. D.; Junior, C. A.; Cândido, B. M. (2022). UAV-Based Vegetation Monitoring for Assessing the Impact of Soil Loss in Olive Orchards in Brazil. *Geoderma Regional*, v. 30. e00543. https://doi.org/10.1016/j.geodrs.2022.e00543

Benvenuto, C. Aterro sanitário – solução técnica ou econômica. Workshop limpeza pública, 2019. Disponível em: http://www.ablp.org.br/userfiles/files/clovis-benvenuto-2019.pdf Acesso em: 15/02/2022

Benvenuto, C. Estabilidade geotécnica de aterros sanitários. I Seminário sobre Geomecânica dos Resíduos Sólidos Urbanos, 2012.

Benvenuto, C. Monitoramento de aterros sanitários. Workshop sobre Resíduos Sólidos Urbanos, 2016. Disponível em: http://www.ablp.org.br/pdf/Clovis-Benvenuto.pdf Acesso em: 15/02/2022

Borrelli, P.; Robinson, D. A.; Panagos, P.; Ballabio, C. (2020). Land use and climate change impacts on global soil erosion by water (2015-2070). *PNAS*. v. 117. n.36. p. 21994-22001. https://doi.org/10.1073/pnas.2001403117

Bruch, A. F. (2020). Avaliação do risco potencial a movimentos de massa no aterro de resíduos sólidos do município de Rio Grande/RS. Trabalho de Conclusão de Curso em Geografia Bacharelado. Universidade Federal do Pelotas. 77 p.

Bruch, A. F.; Cirolini, A.; Thum, A. B. ; Carneiro, M. (2019). Avaliação da Acurácia das Cubagens de Volumes de Mineração através de Levantamentos Convencionais e Fotogramétricos. *Revista Brasileira de Geografia Física*, v. 12, n. 1. p. 283-298. https://doi.org/10.26848/rbgf.v12.1.p283-298

Carrivick, J.F.; Smith, M.W.; Quincey, D.J., (2016) *Structure from motion in the geosciences*: John Wiley & Sons.

Côrrea, J. V.; Almeida, L. C. O.; Ribeiro, F. R. (2018). Avaliação de impacto ambiental do lixão de Leopoldina – MG. In: *Cidade Bem Tratada*: Resíduos Sólidos, Água e Energias Renováveis, 1. Porto Alegre. Anais... Porto Alegre: Unisinos, p.1-11.

Costa, G.; Blanco, C.; Lobato Soares, A.; Cruz, J.; Mendonça, L. (2023). Impacto das mudanças climáticas nas vazões mínimas de referência de pequenas bacias hidrográficas na Amazônia Legal e dentro do arco do desflorestamento. *Revista de Gestão de Água da América Latina*. v.20. 6. https://doi.org/10.21168/rega.v20e6.

Espíndola, I. B.; Ribeiro, W. C. (2020). Cidades e mudanças climáticas: desafios para os planos diretores municipais brasileiros. *Cadernos Metrópole*, São Paulo, 22, n. 48. http://dx.doi.org/10.1590/2236-9996.2020-4802

Fernandes, V.; Cunha, A.; Cuartas, L.; Deusdará-Leal, K.; Costa, L. C.; Broedel, E.; França J.; Alvalá, R.; Seluchi, M.; Marengo, J. (2021). Secas e os impactos na Região Sul do Brasil. *Revista Brasileira de Climatologia*. v.28. http://dx.doi.org/10.5380/rbclima.v28i0.74717.

Ganho, N. (2019). Mudanças climáticas e mudanças na valoração do clima, em Portugal, nos últimos 50 anos. *Acta Geográfica*, v.13(33), 196-208.

Guerra, A. J. T. (2005). Processos Erosivos nas Encostas. In: Guerra, A. J. T.; Cunha, S. B. da (org). *Geomorfologia: Uma atualização de bases e conceitos*. 6. ed. Rio de Janeiro: Bertrand Brasil.

Holben, B.N. (1986) Characteristics of Maximum-Value Composite Images from Temporal AVHRR Data. *International Journal of Remote Sensing*, v.7, 1417-1434. http://dx.doi.org/10.1080/01431168608948945

Hunt, E. R. Jr.; Hively, W. D.; Fujikawa, S. J.; Linden, D. S., Daughtry, C.S.T., Mccarty, G.W. (2010). Acquisition of NIR-Green-Blue Digital Photographs from Unmanned Aircraft for Crop Monitoring. *Remote Sensing***.** v.2(1):290-305. https://doi.org/10.3390/rs2010290

Jara, J. A. L. (2022). *Estimación del indice de vegetación y coeficiente del cultivo para arroz mediante teledetección en la estación experimental vista Florida, Chiclayo* (Dissertação de Mestrado). Universidad Nacional Agraria La Molina.

Jensen, J. (2009). *Sensoriamento Remoto do Ambiente: Uma Perspectiva em Recursos Terrestres*. São José dos Campos, SP: Parêntese editora, 598 p.

Ji, L.; Zhang, L.; Wylie, B. K.; Rover, J. (2011). On the terminology of the spectral vegetation index (NIR - SWIR)/(NIR + SWIR). *International Journal of Remote Sensing*, v. 32 (21): p. 6901–6909, 2011. https://doi.org/10.1080/01431161.2010.510811

Julian, C.; Nunes, J. O. R. (2020). Uso de VANT e geoprocessamento para cálculo de solo erodido em voçoroca localizada no distrito de amadeu amaral. Marília/SP - brasil. *Revista Brasileira De Geomorfologia*, v. 21(4). https://doi.org/10.20502/rbg.v21i4.1818

Liu, W. T. H. (2007). *Aplicações de Sensoriamento Remoto*. Campo Grande: Ed. Uniderp.

Lu, L.; Luo, J.; Xin, Y.; Xu, Y.; Sun, Z.; Duan, H.; Xiao, Q.; Qiu, Y.; Huang, L.; Zhao, J. (2024). A novel strategy for estimating biomass of submerged aquatic vegetation in lake integrating UAV and Sentinel data. *Sci. Total. Environ*. v. 912. https://doi.org/10.1016/j.scitotenv.2023.169404

Mapir (2024). *Environmental Monitoring*. Disponível em: https://www.mapir.camera/en-gb

Marion, F. A.; Andres, J.; Hendges, E. R. Z. (2021) Evolução dos índices de vegetação e sua relação com o estresse hídrico: uma revisão. *Revista GEOFRONTER*. v. 7. P. 01-18.

McFeeters, S.K. (1996). The use of the Normalized Difference Water Index (NDWI) in the delineation of open water features. *International Journal of Remote Sensing*, v.17, n.7, p.1425-1432. https://doi.org/10.1080/01431169608948714

Meinen, B. U.; Robinson, D. T. (2020). Mapping Erosion and Deposition in an Agricultural Landscape: Optimization of UAV Image Acquisition Schemes for SfM-MVS. *Remote Sensing of Environment*, v. 239: 111666. https://doi.org/10.1016/j.rse.2020.111666

Memon, A. A.; Muhammad, S.; Rahman, S.; Haq, M. (2015) Flood monitoring and damage assessment using water indices: A case study of Pakistan flood-2012. *The Egyptian*

Journal of Remote Sensing and Space Science, v. 18 (1): 99-106. https://doi.org/10.1016/j.ejrs.2015.03.003

Nagalli, A. (2005). *Diagnóstico e avaliação dos impactos ambientais de aterros de disposição de resíduos no Estado do Paraná: estudo de caso dos municípios de Jacarezinho e Barra do Jacaré*. Dissertação (Mestrado em Engenharia de Recursos Hídricos e Ambiental) – Universidade Federal do Paraná. Curitiba, 186f.

Nascimento, J. C. F. do. (2007) *Comportamento mecânico de resíduos sólidos urbanos*. Dissertação de mestrado em Geotecnia, EESC/USP.

Nery, C. V. M.; Moreira, A. A.; Fernandes, F. H. S.; Almeida, L. S.; Almeida, R. P. (2014). Utilização do modelo linear de mistura espectral e NDVI para avaliação do comportamento de área desmatada no município de Rio Pardo de Minas/ MG. *Caminhos da Geografia*. v. 15, n. 49, p. 104-112. https://doi.org/10.14393/RCG154923435

Oliveira, T. H.; Silva, J. S.; Machado C. C. C.; Galvíncio, J. D.; Pimentel, R. M. M.; Silva, B. B. (2010). Índice de umidade (NDWI) e análise espaço-temporal do albedo da superfície da bacia hidrográfica do rio Moxotó-PE. **Revista Brasileira de Geografia Física**. v. 03, p. 55-69. https://doi.org/10.26848/rbgf.v3i2.232669

Rouse, J.W.; Haas, R.H.; Schell, J.A.; Deering, D.W. (1973) Monitoring Vegetation Systems in the Great Plains with ERTS (Earth Resources Technology Satellite). *Proceedings of 3rd Earth Resources Technology Satellite Symposium*, Greenbelt, 10-14 December, SP-351, 309-317.

Schuler, A. R. (2010) *Análise do comportamento de um aterro municipal de resíduos sólidos urbanos instrumentado*. Dissertação (Mestrado) – Curso de Pós-graduação em Engenharia Civil, COPPE, Universidade Federal do Rio de Janeiro, Rio de Janeiro, 173f.

Shimazaki, L. R. (2017) *Análise de estabilidade de aterros de resíduos sólidos antigos*. Monografia. Graduação em Engenharia Ambiental. EESC., USP.

Silva, E. R. A. C.; Melo, J. G. S.; Galvíncio, J. D. (2011) Identificação das áreas susceptíveis a processos de desertificação no médio trecho da Bacia do Ipojuca - PE através do mapeamento do estresse hídrico da vegetação e da estimativa do índice de aridez. *Revista Brasileira de Geografia Física*. v. 03 p. 629-649. https://doi.org/10.26848/rbgf.v4i3.232739

Taddia, Y.; Stecchi, F.; Pellegrinelli, A. (2020) Coastal Mapping Using DJI Phantom 4 RTK in Post-Processing Kinematic Mode. *Drones*, v. 4, n. 9, p. 1-19. https://doi.org/10.3390/drones4020009

Tomazelli, L. J.; Villwock, J. A. (1991). Geologia do Sistema Lagunar Holocênico do Litoral Norte do Rio Grande do Sul, Brasil. *Pesquisas*, v. 18(1):13-24.

Verdonk, S. (2015) *Gully volume estimates using UAV Photometry*. Dissertação (Mestrado), University of Utrecht, Utrecht, Países Baixos, p. 80

Villwock, J. A.; Tomazelli, L. J.; Loss, E. L.; DehnhardT, E. A.; Horn, N. O.; Bachi, F. A.; Dehnhardt, B. A. (1986) Geology of the Rio Grande do Sul Coastal Province. In:

Rabassa, J. ed. *Quaternary of South America and Antartic Peninsula*. A. A. Balkema, Rotterdam. 4:79-97.

Wang, R.; Zhang, S.; Pu, L.; Yang, J.; Yang, C.; Chen, J.; Guan, C.; Wang, Q.; Chen, D.; Fu, B.; Sang, X. (2016) Gully erosion mapping and monitoring at multiple scales based on multi-source remote sensing data of the Sancha river catchment, Northeast China. *ISPRRS Int. Geo-Inf***.** v. 5, n° 11, 200. https://doi.org/10.3390/ijgi5110200.

Zhou, Y.; Daakir, M.; Rupnik, E.; Pierrot-Deseilligny, M. (2020) A two-step approach for the correction of rolling shutter distortion in UAV photogrammetry. *ISPRS Journal of Photogrammetry and Remote Sensing*, v. 160, p. 51–66. https://doi.org/10.1016/j.isprsjprs.2019.11.020

Zúñiga, A. C. E.; Vásquez, J. Ñ. (2021). Detection and identification of high Andean lant communities, Wetlands and Tolar de Puna Seca by means of RGB and NDVI orthophotos in "Unmanned Aerial Systems" drones. *Scientia Agropecuaria*, [s. l.], v. 12, n. 3, p. 291–301. https://doi.org/10.17268/sci.agropecu.2021.032.